Development of an IrO_x Micro pH Sensor Array on Flexible Polymer Substrate

Wen-Ding Huang, Jianqun Wang, Thermpon Ativanichayaphong, Mu Chiao* and J.C. Chiao

Department of Electrical Engineering, University of Texas at Arlington, TX, USA
*Department of Mechanical Engineering, University of British Columbia, Vancouver, BC, Canada

ABSTRACT

pH sensor is an essential component used in many chemical, food, and bio-material industries. Conventional glass electrodes have been used to construct pH sensors, however, have some disadvantages in specific applications. It is difficult to use glass electrodes for *in vivo* biomedical or food monitoring applications due to size limitation and no deformability. In this paper, we present design and fabrication processes of a miniature iridium oxide thin film pH sensor array on flexible polymer substrates. The amorphous iridium oxide thin film was used as the sensing material. A sol-gel dip-coating process of iridium oxide film was demonstrated in this paper. A super-Nernstian response has been measured on individual sensors of the array with a slope of -71.6 ± 3 mV/pH at 25°C within the pH range between 2.83 and 11.04.

Key words: miniature pH sensor array, flexible polymer substrate, sol-gel process, electro-plating process, smart litmus paper

INTRODUCTION

To achieve small sizes and reliable performance in pH sensing applications, ion-sensitive field-effect transistor (iSFET) pH sensors [1,2], optical fiber pH sensors [3,4], hydrogel film pH sensors [5] and solid-sate pH sensors [6,7] have been proposed and demonstrated. Most of the sensors were based on rigid substrates so they were not flexible to deform on a curved surface or fit into a small space. The mechanical rigidity also limits their long-term uses in tissues due to Young's Modulus mismatch between devices and tissues causing localized scar tissue formation such as the ones seen in neuronal implants [8,9]. Deformable, biomechanically-compatible and implantable pH sensors then are needed.

Polymer-based substrate provides chemical-resistant, corrosion-resistant and deformable properties making them a popular choice for biochemical sensors. Meanwhile, planarization ability and thermal stability of polymers are suitable to utilize existing IC fabrication techniques in the processes. The polymer fabrication also provides possibility for versatile micromachined structures. 3-D structures can be made by plasma etching, deep reactive ion etching, photolithography and hot embossing techniques [10,11] for increasing sensitivity and circuitry integration. We chose Kapton polyimide film as the sensor substrate for this preliminary investigation based on our previous experience in making circuitry on Kapton [12].

Sol-gel fabrication technology has shown wide applications in devices [13,14] due to its advantages over other deposition methods [15-17] such as simpler processes, lower costs and robustness to harsh environments [18]. Sol-gel processes for pH sensors have been demonstrated and shown excellent performance on rigid substrates [19]. The fabrication techniques, however, need to be reinvestigated when used on flexible substrates.

In this paper, we developed a miniature pH sensor array based on flexible Kapton substrates using iridium oxide sol-gel techniques. The purpose was to develop a smart electronic litmus paper. The amorphous iridium oxide thin film was formed by dip-coating and sequential heat treatment techniques [19] that have been used in industry. We investigated design considerations, fabrication processes and experimental results of the deformable miniature pH sensors.

Nanosensors and Microsensors for Bio-Systems 2008, edited by Vijay K. Varadan,
Proc. of SPIE Vol. 6931, 693104, (2008) · 0277-786X/08/$18 · doi: 10.1117/12.775856

PRINCIPLE

There are three possible mechanisms on pH-dependent redox equilibriums between two oxidation states of iridium oxide [20]:

$$Ir_2O_3 + 6H^+ + 6e^- \leftrightarrow 2Ir + 3H_2O \quad [1]$$

$$IrO_2 + 4H^+ + 4e^- \leftrightarrow Ir + 2H_2O \quad [2]$$

$$2IrO_2 + 2H^+ + 2e^- \leftrightarrow Ir_2O_3 + H_2O \quad [3]$$

$$E = E^0 - 2.303\frac{RT}{F}pH = E^o - 59.16pH \quad [4]$$

where E^0 is the standard electrode potential (926 mV), F is the Faraday constant (96,487 coul/equivalent), and R is the gas constant with a value of 8.314 joules/(°K·mol). The value RT/F is 25.688 at 25°C. The pH potential sensitivity will be –59.16 mV/pH regarded as the Nernstian potential response [20-22]. Various fabrication techniques have been demonstrated showing near-Nernstian, Nernstian and super-Nernstian responses [21]. Generally speaking, electrochemical deposition and electro-deposition produced super-Nernstian responses with higher sensitivity in sensor performance while sputtered coating and thermal method produced near-Nernstian or Nernstian sensitivity.

SENSOR FABRICATION

Fig.1 shows the fabrication steps. The polyimide polymers were washed with acetone in an ultrasonic bath to remove contamination. Positive photoresist S1813 was spun on top of the polymers at 3000 rpm for 30 seconds, followed by 100°C hot-plate baking for 1 minute. The working electrode patterns were exposed through a photomask for 9.5 seconds. Post exposure bake was performed at 100°C for 1 minute. The samples were then

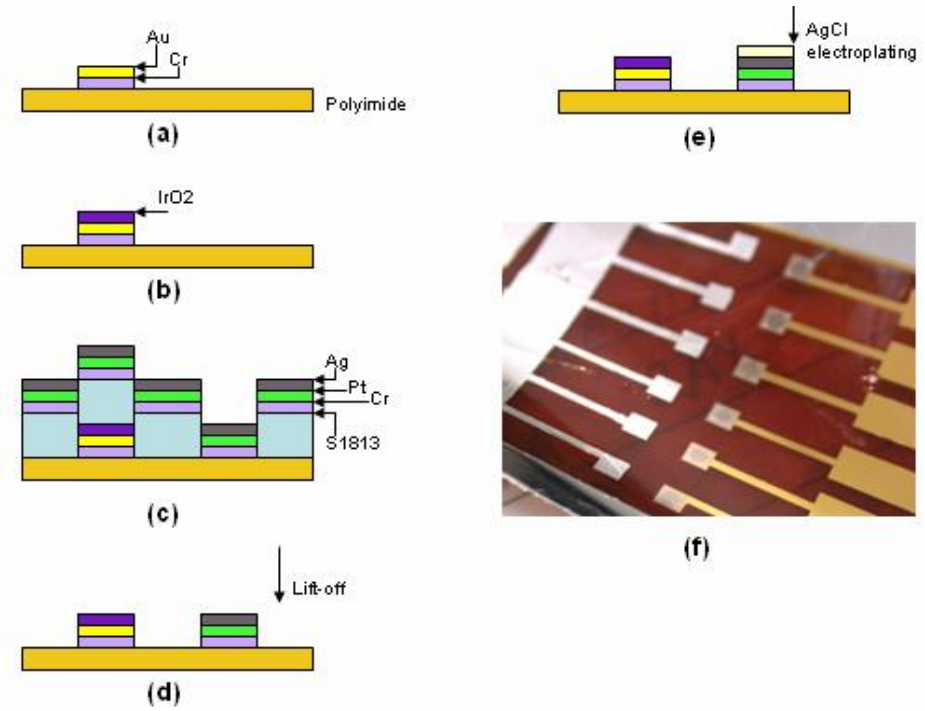

Figure 1 Fabrication processes: (a) Cr and Au deposition, (b) $IrCl_4$ sol-gel process after SU-8 deposition as the sacrificial layer, (c) Cr, Pt and Ag deposition with S1813 as the sacrificial layer, (d) lift-off process result, (e) AgCl electroplating. (f) A photo of the sensor array.

developed, followed by deionized (DI) water rinse and nitrogen air drying.

A 70-Å thick chromium and 1500-Å thick gold layer was deposited using an electron-beam evaporator. The chromium layer served as an adhesion layer. The Cr-Au layer showed excellent conductivity and stability in our acid tests later. The sample was soaked in acetone with ultrasonic agitation for metal lift-off. Due to uncertainty of excessive evaporation heating in the evaporator, the S1813 may be partially cured making it difficult for lift-off. Extra time to soak then might be needed.

An SU-8-100 photoresist layer was applied as the sacrificial layer on top of the working electrode metals. The spin cycle was set at 500 rpm/sec for ten seconds with an acceleration rate of 100 rpm/s, then at 3000 rpm/s for 30 seconds with an acceleration rate of 300 rpm/s. The sample was baked at 65°C for 10 minutes and 95°C for 30 minutes. The electrode patterns were defined and the sample was baked for 3 minutes at 65°C and then 10 minutes at 95°C. The sample was developed and dried. The thickness of the SU-8 layer was measured around 95 to 105 μm by a profilometer.

In this work, we aimed to demonstrate a simple iridium oxide thin film sol-gel process. The sol-gel coating solution was based on the recipe for rigid substrates described in [23]. One gram of anhydrous iridium chloride ($IrCl_4$) was dissolved in 42 ml of ethanol (C_2H_5OH) followed by adding 10 ml of acetic acid (CH_3COOH) in the solution. The solution was stirred continuously by a magnetic rod at the bottom of the beaker for at least one hour. A thin layer on the flexible substrate was formed by dip coating at a 2 cm/min withdraw rate in the solution. A higher withdraw rate in the dip coating process would produce lower crystallinity [24]. After dip coating, the sample was baked at 150°C for at least 1 hour. The SU-8 layer was stripped off after baking. The sample was treated in an oven purged with inert gas and with a heating profile starting at 25°C and increasing to 300°C in a period of 2 hours. The

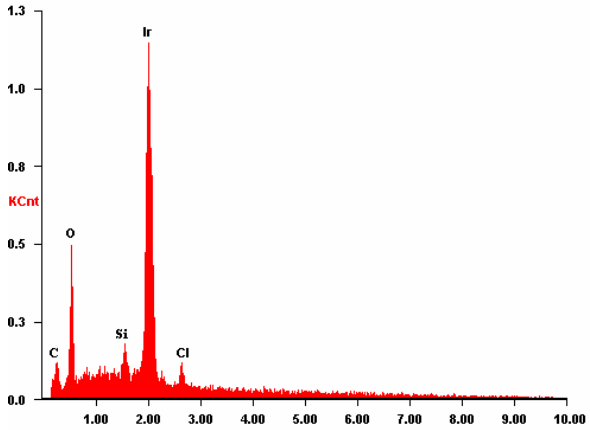

Figure 2 Energy-dispersive x-ray analysis result of the sol-gel IrO_x film.

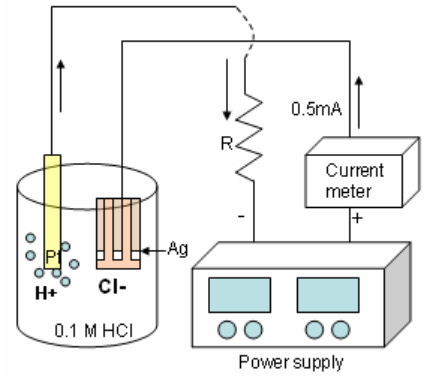

Figure 3 Electroplating setup for the AgCl reference electrodes.

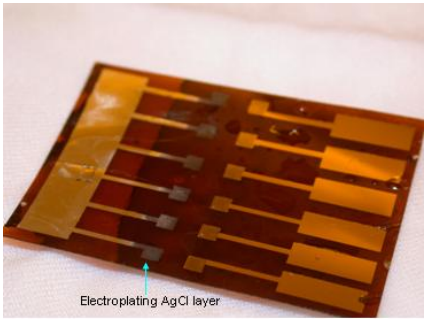

(a)

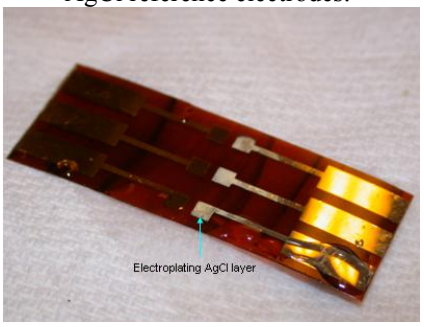

(b)

Figure 4 AgCl electroplating layer (a) before and (b) after KCl saturation process.

temperature stayed at 300°C for another 5 hours. To obtain amorphous iridium oxide film, the surface needed to be heated at a temperature between 300°C and 350°C [25]. We have tested the film crystallinity with treatment temperatures at 350°C and 550°C. The oven then was cooled down gradually in 10 hours to 25°C.

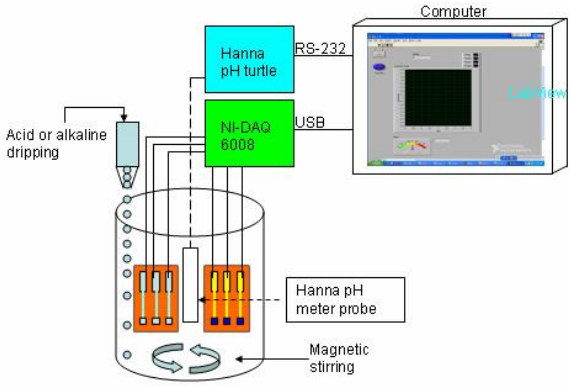

Figure 5 pH titration and measurement setup.

The thickness of the iridium oxide thin film was around 0.4~0.6μm measured by a KLA-Tencor profilometer. The sample was prepared for energy-dispersive x-ray analysis using the EDAX 4000 Electron Dispersive Analysis System in a Zeiss Supra 55 VP scanning electron microscope (SEM)**.** Fig. 2 shows the energy-dispersive x-ray analysis result of the sol-gel IrO_x film. The ratio between iridium and oxygen was measured 2.4. Some other small amounts of elements such as chlorine, silicon and carbon detected were probably due to contamination from the solution and the device carrier under the sensor in the SEM. The Kapton film was carried on a silicon substrate.

70Å thick chromium, 60Å thick platinum and 3000Å thick silver layers were deposited by electron-beam evaporation. Photolithography and lift-off processes were applied to define the reference electrodes. The platinum layer showed good adhesion for the silver layer during the following electroplating processes.

Fig. 3 shows the electroplating setup for the Ag/AgCl reference electrodes. Electrochemical anodization process was applied on anodic silver electrodes with a platinum cathode electrode in 0.1M HCl solution. An electrical current of 0.5mA was applied for 5 seconds. During the electrolysis, a brown silver chloride layer was formed on the silver surface as shown in Fig. 4(a). The electrode surface was rinsed in DI water and immersed in 3M KCl solution for 24 hours in order to reach a stable potential [26]. Fig. 4(b) shows the electrodes after the saturation process. The AgCl thickness was measured as 1.5μm by a KLA-Tencor profilometer.

CHARACTERIZATION

Fig. 5 shows the measurement setup for our micro pH sensors. An NI-DAQ 6008 USB card with a LabVIEW program were used for analog potential recording. A commercial Hanna pH meter was used to verify the pH values of solutions. Our pH sensor array was clipped by flat gator clamps and connected to the DAQ card. The sensor array was immersed in acid or alkaline based diluted solution stirred with a magnetic rod in the beaker. We used hydrochloric acid for acidic titration tests. NH_3 and KOH were used for alkaline titration tests. The Hanna pH meter was placed in the solution and connected to its signal processing card. Both the potential from our sensor array and the pH level from the Hanna pH meter were recorded in a computer simultaneously.

RESULTS AND DISCUSSION

X-ray diffraction patterns and scanning electron microscope analysis

In order to confirm the iridium oxide thin film formation, x-ray diffraction (XRD) patterns were performed using Siemens D-500 x-ray diffractometer. Fig. 6 shows the XRD patterns at annealing temperatures of 350°C and 550°C. The crystallization of iridium oxide normally begins at 400°C [27]. We compared the results with 5-hour 350°C and 550°C heating treatments. The iridium oxide crystal structure from XRD patterns shown in Fig. 6 agreed with the results shown in the literatures [24, 25]. The data showed a lower temperature treatment produced weaker diffraction due to lower crystallinity. This indicated our iridium oxide thin film was close to amorphous and fine grain structures. Our data showed clearly stronger diffraction peaks for the 550°C annealing temperature. The wide line widths and peak shifts were probably due to local disorders and/or micro-crystallinity [24] in the film.

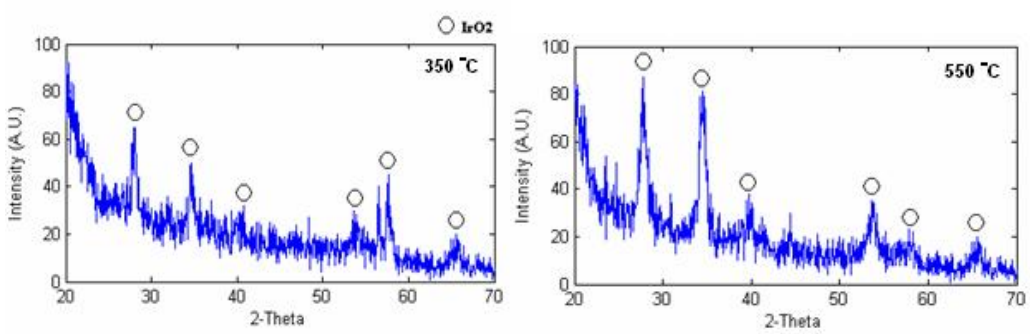

Figure 6 XRD patterns for IrO_x with thermal treatment at (a) 350°C and (b) 550°C.

Fig. 7 shows the IrO_x surfaces with (a) 350°C and (b) 550°C treatments using a ZEISS Supra 55 VP scanning electron microscope (SEM). The iridium oxide thin film crystallized at 550°C and the surface was cracked in multiple places across the film. With 350°C thermal treatment, the surface was uniformly smooth without crystallization or cracks. In our sensor applications, a uniform and stable sensing film surface will be required. These experiments showed a 350°C heat treatment would provide the required film quality.

Sensor Performance

A titration test was performed to investigate the response time of our pH sensor. The titration test starts from acidic to alkaline solutions with KOH dripping into the beaker. The response time is defined as the time required to reach 90% of the equilibrium value [28]. Fig. 8 shows the results with two transition steps of pH changing from pH=2 to pH=6 and from pH=6 to pH=12. Two electrodes in an array were tested simultaneously. The response times were about 6 seconds. The response times measured also included the mixing time of the dripped liquid with the base solution.

A linear potential response of the IrO_x pH sensor was confirmed by pH titration tests. KOH was dripped into diluted HCl solution for titration. Shown in Fig. 9, our pH sensor demonstrated a linear super-Nernstian response [22] with a sensitivity of –71.6 mV/pH from pH=2.83 to pH=11.04 at 25°C.

Fig. 10 shows potential responses of two IrO_x sensors to pH changes in a series of different pH levels. The diluted KOH-based solution was titrated by 1M HCl dripping from pH=11.9 to pH=3. The IrO_x film electrodes on flexible substrates performed coordinately with different pH levels. The potential responded quickly when the

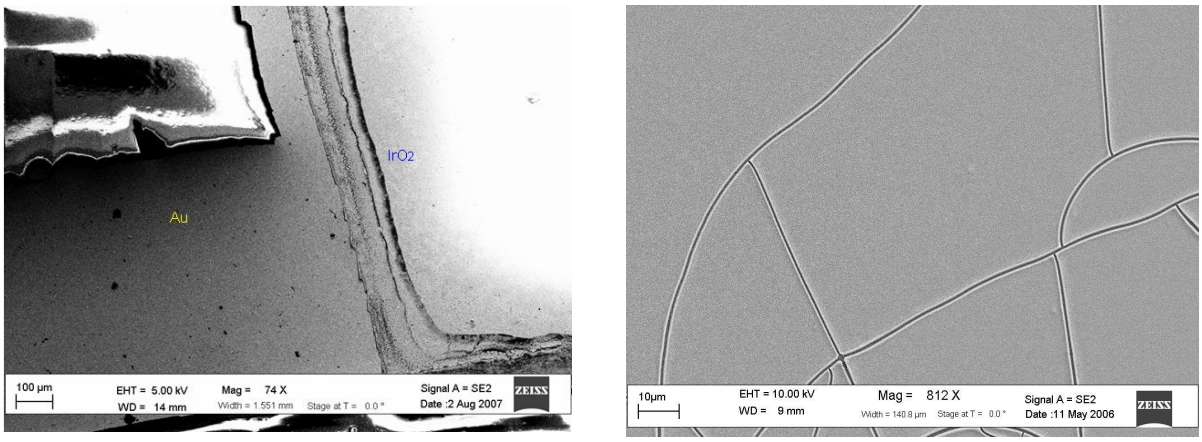

(a) (b)

Figure 7 SEM photos for IrO_x treated at (a) 350°C and (b) 550°C.

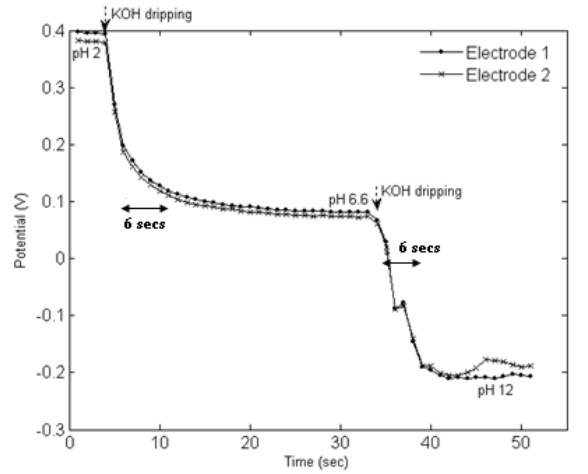

Figure 8 Response times of our pH sensor array from pH=2 to pH=12.

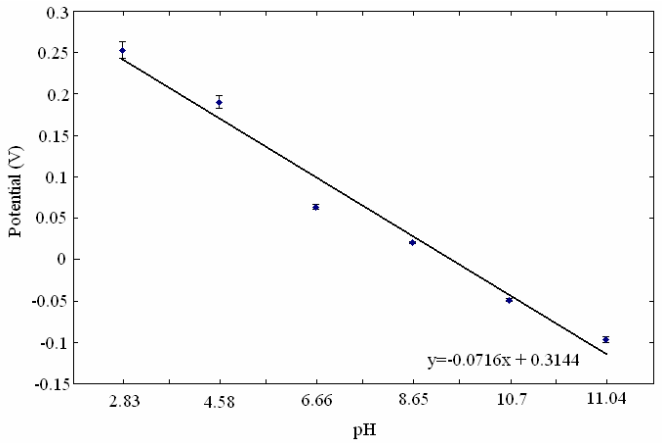

Figure 9 Linear potential response of our pH sensor from pH=2.83 to pH= 11.04.

titration solution was dripped into the beaker. As the solution been mixed continuously by the magnetic stirrer, the potential slowly settled to a stable value while average pH values were recorded from the pH meter. A constant DC potential shift by a resister was added to one electrode in order to distinguish the potential curves from two different electrodes. These two sensors were fabricated at two different batches but the potential responses were almost identical. This experiment also showed the reproducibility of our sol-gel fabrication processes.

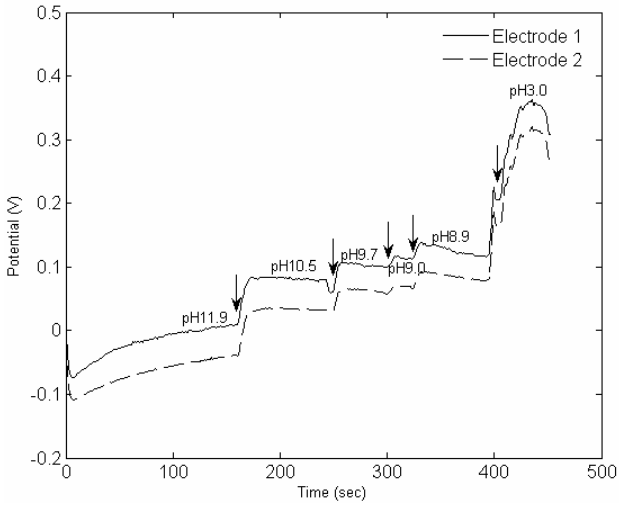

Figure 10 Step potential responses from our pH sensors.

Without calibration done to the sensor electrodes, two IrO_x electrodes in an array were tested in a 30-minute dynamic titration experiment in which HCl and KOH solutions were added separately and pseudo-randomly into the beaker while stirred with a magnetic rod at the bottom of the beaker. Fig. 11 show the potential changes compared with the pH values recorded from the commercial pH meter. This test verified repeatability and reversibility of our pH electrodes. The potential variations from our sensor electrodes responded to the pH value measured. Our sensor electrodes responded quicker than the pH meter. The results however showed potential drifts and the drifts increased as more titration solution was dripped into the base solution. This may be due to the potential interference from the glass electrode of the commercial pH meter to the sensing and reference electrodes in our sensor. As more charged particles were added into the solution, the impedance of the solution changed and fluctuated the potentials.

To investigate the reference electrode performance, a commercial AgCl electrode purchased from Warner Inc. and our electroplated Ag/AgCl reference electrode were used with the same IrO_x electrode in the dynamic pH titration. As shown in Fig. 12, the electroplated reference electrodes provided mostly the same potential responses with those from the commercial AgCl electrode.

CONCLUSIONS

A flexible iridium oxide pH sensor array was fabricated with sol-gel processes. The sol-gel technique provided simple and economical fabrication processes. The amorphous iridium oxide thin film was formed on Kapton, confirmed by XRD, SEM and EDAX analysis. Ag/AgCl reference electrodes were made by electroplating with a

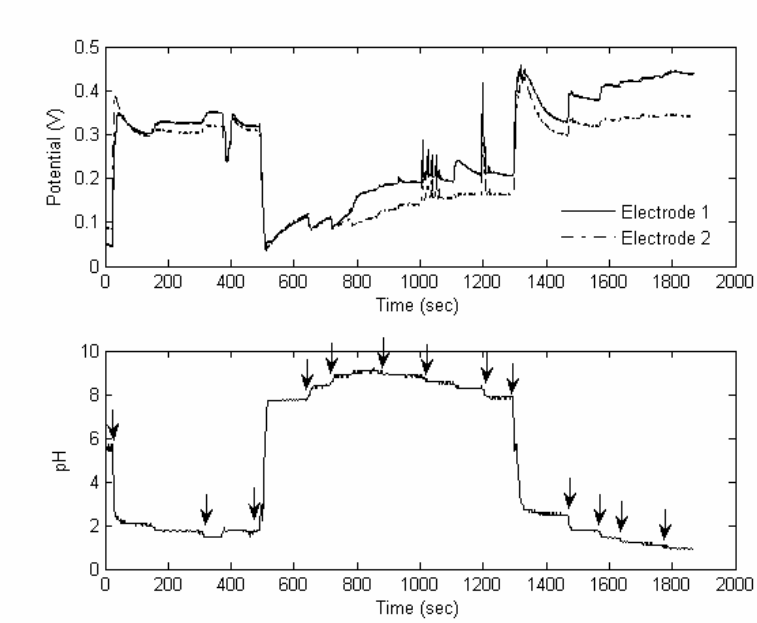

Figure 11 Dynamic pH titration test. The arrows indicate the events when acidic or alkaline solution was added.

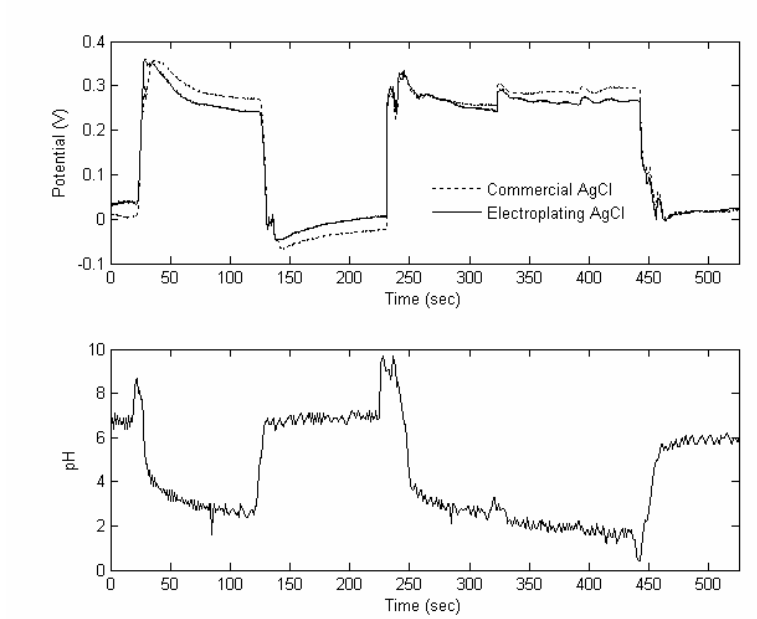

Figure 12 Comparison of commercial and our electroplated Ag/AgCl reference electrodes.

KCl saturation procedure. A super-Nernstian potential was measured and matched with the theory of ion selective electrodes. The pH sensor performed high sensitivity, repeatability and reversibility in dynamic titration tests.

The flexible pH sensors provide many potential applications in biomedical, biological, food monitoring industries. The smart litmus paper can be used electronically offering broader applications than a conventional pH meter.

ACKNOWLEDGEMENT

The authors appreciated the research funding support by the AFOSR #FA-9550-06-0413.

REFERENCES

[1] Yi Liu, Tianhoung Cui, "Ion-sensitive field-effect transistor based pH sensors using nano self-assembled polyelectrolyte/nanoparticle multilayer films," *Sensors and Actuators B*, Vol. 123, pp. 148-152, Aug. 2006.

[2] Jinghong Han, Dafu Cui, Yating Li, *et al.*, "A gastroesophageal tract pH sensor based on the H-ISFET and the monitoring system for 24 h," *Sensors and Actuators B*, Vol. 66, pp. 203-204, July 2000.

[3] Otto S. Wolfbeis, "Fiber-optic chemical sensors and biosensors," *Anal. Chem.*, Vol. 76, pp. 3269-3284, 2004.

[4] Saying Dong, Ming Luo, Gangding Peng, and Wenhua Cheng, "Broad range pH sensor based on sol–gel entrapped indicators on fiber optic," *Sensors and Actuators B: Chemical*, Vol. 129, pp. 94-98, Jan. 2008.

[5] Gerald Gerlach, Margarita Guenther, *et. al*, "Chemical and pH sensors based on the swelling behavior of hydrogels," *Sensors and Actuators B*, Vol. 111-112, pp. 555-561, Nov. 2005.

[6] Agner Fog, Richard P. Buck, "Electronic semiconducting oxides as pH sensors," *Sensors and Actuators*, Vol. 6, pp. 137-146, 1984.

[7] Patrick J. Kinlen, John E. Heider, and David E. Hubbard, "A solid-state pH sensor based on a Nafion-coated iridium oxide indicator electrode and a polymer-based silver chloride reference electrode," *Sensors and Actuators B*, Vol. 22, pp. 13-25, 1994.

[8] Roy Biran, David C. Martin and Patrick A. Tresco, "Neuronal cell loss accompanies the brain tissue response to chronically implanted silicon microelectrode arrays," *Experimental Neurology*, Vol. 195, pp. 115-126, 2005.

[9] Vadim S. Polikov, Patrick A. Tresco and William M. Reichert, "Response of brain tissue to chronically implanted neural electrodes," *Journal of Neuroscience Methods*, Vol. 148: pp.1-18, 2005.

[10] "A Distributed MEMS Phase Shifter on A Low-Resistivity Silicon Substrate," Jianqun Wang, Thermpon Ativanichayaphong, Wen-Ding Huang, Ying Cai, Alan Davis, Mu Chiao and J.-C. Chiao, *Sensors and Actuators A: Physical*, *In Press. Available online January 5, 2008.*

[11] "Plastic 95-GHz Rectangular Waveguides by Micro Molding Technologies," F. Sammoura, Y. C. Su, Y. Cai, C.-Y. Chi, B. Elamaran, Liwei Lin and J.-C. Chiao, *Sensors & Actuators,* Vol. 127, pp. 270-275, 2006.

[12] "Fabrication techniques for RF transmission lines on polymer substrates," Jianqun Wang, Ying Cai, Thermpon Ativanichayaphong, Mu Chiao and J.-C. Chiao, *Microelectronics, MEMS, and Nanotechnology Symposium, Microelectronics: Design, Technology, and Packaging Conference*, Brisbane Australia, Dec. 11-14, 2005.

[13] Paula C.A. Jer'onimo, Alberto N. A., M. Conceic, and B.S.M. Montenegro, "Optical sensors and biosensors based on sol–gel films," *Talanta*, Vol. 72, pp. 13-27, 2007.

[14] N. Carmona, E. Herrero, J. Llopis, and M.A. Villegas, "Chemical sol-gel-based sensors for evaluation of environmental humidity," *Sensors and Actuators B*, Vol. 126, pp. 455-460, 2007.

[15] J. V. Dobson, P. R. Snodin and H. R. Thirsk, "EMF measurements of cells employing metal—metal oxide electrodes in aqueous chloride and sulphate electrolytes at temperatures between 25–250°C," *Electrochimica Acta.,* Vol. 21, pp. 527-533, 1976.

[16] T. Katsube, I. Lauks and J. N. Zemel, "pH-sensitive sputtered iridium oxide films," *Sensors and Actuators*, Vol. 2, pp. 399-410, 1981.

[17] M.F. Yuen, I. Lauks, and W.C. Dautremont-Smith, "pH dependent voltanmmetry of iridium oxide films," *Solid State Ionics*, Vol. 11, pp. 19-29, 1983.

[18] G. Beltran-Perez, F. Lopez-Huerta, S. M.-Aguirre, J. Castillo-Mixcoatl, R. Palomino-Merino, R. Lozada-Morales, and O. Portillo-Moreno, "Fabrication and characterization of an optical fiber pH sensor using sol–gel deposited TiO2 film doped with organic dyes," *Sensors and Actuators B*, Vol. 120, pp. 74-78, 2006.

[19] C. Jefferey Brinker, George W. Scherer, *Sol-Gel Science: The physics and Chemistry of Sol-Gel Processing*, pp.788-798, Academic Press, Boston, 1990.

[20] M. Pourbaix, "Atlas of electrochemical equilibria in aqueous solutions," *National Association of Corrosion Engineers*, pp. 374-377, 1974.

[21] Sheng Yao, Min Wang, and Marc Madou, "A pH electrode based on melt-oxidized iridium oxide," *Journal of the elecvtrochemical society*, Vol. 148, pp. 29-36, 2001.

[22] Erno Pungor, “The theory of ion-selective electrodes,” *The Japan society for analytical chemistry*, Vol. 14, pp. 249-256, 1998.

[23] K. Nishio, Y. Watanabe, T. Tsuchiya, “Preparation and properties of electrochromic iridium oxide thin film by sol-gel process,” *Thin Solid Films*, Vol. 350, pp. 96-100, 1999.

[24] R.H. Horng, D.S. Wuu, L.H. Wu, and M.K. Lee, “Formation Process and Material Properties of Reactive Sputtered IrO2 Thin Films,” *Superficies y Vacio,* Vol. 9, pp. 139-142, 1999.

[25] Akiyoshi Osaka, Toru Takatsuna, Yoshinari Miura, “Iridium oxide films via sol-gel processing,” *Non-Crystalline Solids*, Vol. 178, pp. 313-319, 1994.

[26] A W J Cranny, J K Atkinson, "Thick film silver–silver chloride reference electrodes," *Meas. Sci. Technol*, pp.1557-1565, 1998.

[27] Keishi Nishio, Toshio Tsuchiya, "Electrochromic thin films prepared by sol-gel process", *Solar Energy Materials& Solar Cells*, Vol. 68, pp. 279-293, 2001.

[28] Haley R. Clark, Timothy A. Barbari, “Modeling the response time of an in vivo glucose affinity sensor,” *Biotechnol. Prog.*, Vol. 15, pp. 259-266, 1999.